Graphene Plasmon Cavities Made With Silicon Carbide

Ke Li,[†,‡,§] Jamie M. Fitzgerald,[‡,§] Xiaofei Xiao,[*,‡,§] Joshua D. Caldwell,[¶] Cheng Zhang,[†] Stefan A. Maier,[‡] Xiaofeng Li,[*,†] and Vincenzo Giannini[‡]

College of Physics, Optoelectronics and Energy, Collaborative Innovation Center of Suzhou Nano Science and Technology, Key Lab of Modern Optical Technologies of Education Ministry of China, Soochow University, Suzhou 215006, China., The Blackett Laboratory, Imperial College London, London SW7 2AZ, United Kingdom, and US Naval Research Laboratory, 4555 Overlook Avenue SW, Washington DC 20375, USA

E-mail: xx2215@ic.ac.uk; xfli@suda.edu.cn

Abstract

We propose a simple way to create tunable plasmonic cavities in the infrared using graphene films suspended upon a SiC grating and present a numerical investigation, using the finite element method, on the absorption properties and field distributions of such resonant structures. We find at certain frequencies within the SiC Reststrahlen band that the structured SiC substrate acts as a perfect reflector, providing a cavity effect by establishing graphene plasmon standing waves. We also provide clear evidence of strong coupling phenomena between the localized surface phonon polariton

[*]To whom correspondence should be addressed

[†]College of Physics, Optoelectronics and Energy, Collaborative Innovation Center of Suzhou Nano Science and Technology, Key Lab of Modern Optical Technologies of Education Ministry of China, Soochow University, Suzhou 215006, China.

[‡]The Blackett Laboratory, Imperial College London, London SW7 2AZ, United Kingdom

[¶]US Naval Research Laboratory, 4555 Overlook Avenue SW, Washington DC 20375, USA

[§]These authors contributed equally to this work (K.L., J.M.F. and X.X.).

resonances in the SiC grating with the graphene surface plasmon cavity modes, which is revealed by a Rabi splitting in the absorption spectrum. This paves the way to build simple plasmonic structures, using well known materials and experimental techniques, that can be used to excite graphene plasmons efficiently, even at normal incidence, as well as explore cavity quantum-electrodynamics and potential applications in infrared spectroscopy.

Keywords

graphene, surface plasmons, silicon carbide, surface phonon polaritons, Rabi splitting

1 Introduction

Graphene is a 2D single-atom thick layer of carbon and after the experimental proof of existence in 2004,[1] its remarkable physical properties have led to one of the most prolific areas of research in nanoscience. In particular, its extreme 2D geometry and distinct bandstructure leads to novel interaction with light and has resulted in immense interest from the plasmonics and nano-optics communities.[2] Doped graphene supports collective oscillations of the free carriers known as surface plasmon polaritons (SPPs) that can be either propagating or localised[2,3] and has been recognized as a suitable alternative to noble metals in the field of plasmonics. These plasmonic modes are characterized by large field confinement (plasmon wavelengths a hundred times smaller than the free space wavelength has been demonstrated at mid-IR frequencies[4]) and enhancements and is particularly appealing in graphene due to the tunability of the Fermi energy via chemical doping or electrical gating. Optical gaps of up to 2 eV (which corresponds to $E_F \sim 1\ eV$) can be created.[5] This paves the way for cheap, reliable and ultrafast optical modulators. At THz and IR frequencies graphene plasmons have been conclusively demonstrated by a number of different experimental techniques including scanning near-field microscopy,[6–8] optical far field[9] and electron energy-loss

spectroscopy.[10]

SiC is a polar dielectric that supports subdiffraction confinement of light using the excitation of surface phonon polaritons (SPhPs) which result from the coupling of a photon with the collective oscillation of the polar lattice atoms.[11] Due to the energy scale of optic phonons, the Reststrahlen band (a narrow and material-dependent frequency range bounded by the longitudinal optic (LO) and transverse optic (TO) phonon frequencies) inherently occurs within the IR to THz regime where polar dielectrics act as an optical metal i.e. they exhibit high reflectivity and negative real part of the dielectric function. The long phonon lifetimes (picoseconds), as compared to electron scattering times in metals (10s of femtoseconds), means the imaginary part of the dielectric function can be orders of magnitude smaller than for noble metals, leading to low loss systems with high quality factors and narrow linewidths.[11] As previously shown, nanostructuring SiC results in localised surface phonon polaritons (LSPhPs) with a high Q and strong field confinement.[12,13] SiC also has a large band-gap and high thermal, mechanical and chemical stability making it highly suitable for a number of applications.

In this work, we explore the coupling between SiC LSPhPs and graphene SPPs and

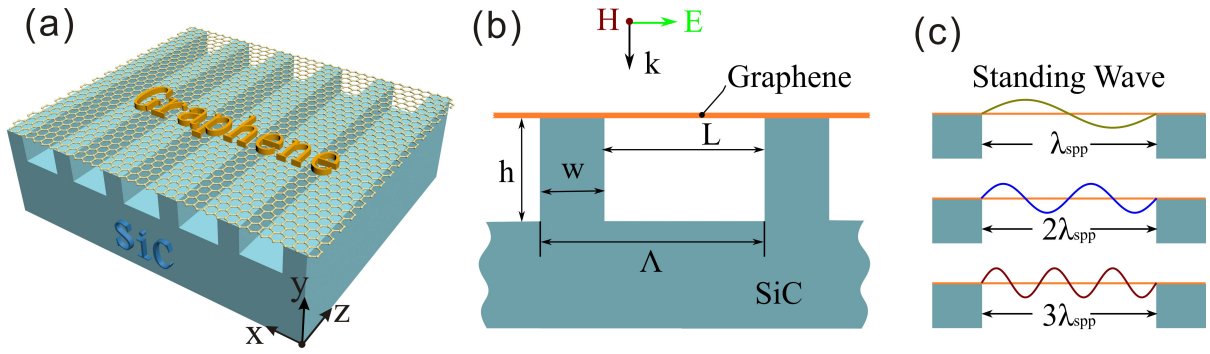

Figure 1: Schematics of the SiC grating plus graphene plasmonic device. (a) Three-dimensional view of the whole structure and (b) cross-sectional view, the incident light is TM polarized normal incident in the air, where Λ is the grating period, w is the width of the grating ridge, L is the width of the grating groove, h is the grating height. (c) Sketch of the standing waves of Graphene SPPs resonance in grating cavity.

explore the unique properties of the hybrid modes[14] which combine positive characteristic of the graphene SPPs (large light confinement, tunable) and SiC LSPhPs (low loss). We con-

sider a single-layer graphene sheet on top of a SiC cavity. Structuring the SiC[12,13] allows for the excitation of both the graphene SPP and a LSPhP in the SiC. This is convenient as the difficulty in nanofabrication of graphene devices, as well as the large momentum mismatch between graphene SPPs and incident light, means creating graphene based resonators, which can be excited at normal incidence, is challenging. A numerical investigation, using finite element analysis method from COMSOL Multiphysics, on the absorption properties and field distributions of this system in the IR is reported. At frequencies in the Reststrahlen band, but away from the LSPhP resonances, the SiC acts as like a 'perfect conductor' and, at certain grating groove lengths, a plasmon standing wave is set up. Here, by perfect conductor we simply mean that the real part of the permittivity is extremely large and negative (small field penetration), we assume that the SiC is undoped and hence is not conductive. This setup is a different way to excite localised graphene plasmons, and achieve strong resonant absorption, without using nanoribbons. Note that whilst we consider the cavity as part of a periodic structure (i.e. a grating which is convenient for experiments and numerical simulations), we are not considering the excitation of modes using diffraction. The necessary momentum is provided by the abrupt breaking of the symmetry of the cavity, not via the periodicity [i].

There is a lot of interest on the coupling of surface phonons and graphene plasmons, which becomes important at the mid-IR for typical polar dielectric substrates like SiC[15,16] and SiO_2.[6,17,18] It has also been demonstrated in graphene/h-BN heterostructures,[4,19–22] and thin layers of surface absorbed polymers.[23] Recently the interaction of localised plasmons in a gold antenna with a SiO_2 coating and substrate has been explored and it was found that strong coupling between the modes leads to a transparency window.[24] We find, near the LO phonon frequency, a strong interaction between the LSPhPs and the graphene plasmons leading to Rabi splitting, signalling the coherent energy transfer between the two coupled

[i]Proof of this is that the modes we explore are not reproduced by the equation $k_{spp} = N\frac{2\pi}{\Lambda}$ where N is the diffraction order and Λ is the grating period. We consider a grating because it simplifies the calculation but similar results would be obtained by a single cavity.

modes.[25,26] The high quality factor Q and small effective volume V of the hybrid modes makes this a suitable system for cavity quantum-electrodynamics[27] where one is interested in the strong mixing of light and individual emitters. In photonic cavities the modal volume is on the order of λ^3 but by using localized surface plasmons (LSPs) and/or LSPhPs one can confine light fields evanescently and achieve subdiffraction modal volume. Using hybrid modes to tailor the spectral and spatial profile of localised plasmons to aid strong coupling to emitters has been demonstrated.[28] By picking suitable constituent modes that have complimentary characteristics, the Q/V ratio, which is proportional to the Purcell factor, can be increased to enhance strong light-matter interactions with emitters. Our work provides a potential method to efficiently excite unique hybrid modes for confining, and manipulating light, and could pave the way for applications in tunable, broadband molecular spectroscopy in the THz and IR range.[29] Furthermore the device potentially provides a new system in which to study cavity quantum-electrodynamics. The high quality factor plus the small modal volume makes this system a very suitable platform for inducing and exploring strong light-matter interactions.

2 Results and Discussions

In figure 1 we show the system to be studied. It is composed of a monolayer graphene sheet disposited on a SiC grating, we assume the two are touching. The graphene sheet is located on the $x-z$ plane with the grating periodic in the x direction. The incident light propagates in the y direction from above and is normal to the graphene surface, it is transverse magnetic (TM) which can excite SPPs above the grating in the graphene layer. The grating's height, period, ridge width and groove width are respectively represented by the letters h, Λ, w and L (see figure 1b). The graphene thickness in the simulations is 0.5 nm, which we have checked is converged for all results. The cavity supporting the graphene SPPs is given by

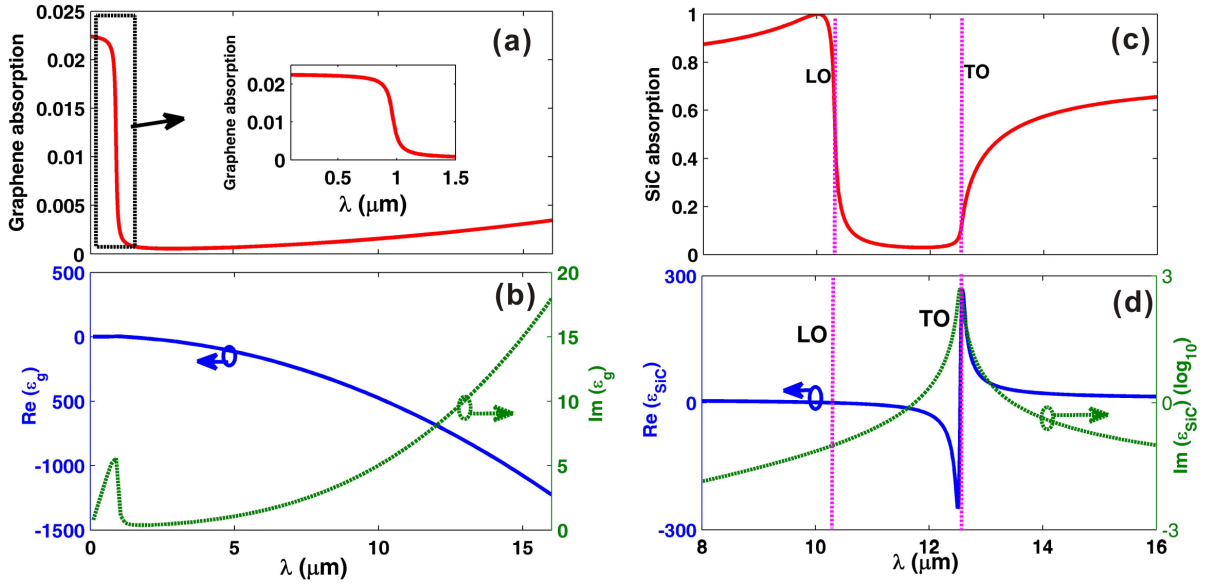

Figure 2: Material properties of single layer graphene in air ((a) and (b)) and bulk SiC ((c) and (d)), the graphene's chemical potential is $E_F = 0.64\ eV$ and carrier mobility $\mu = 10000\ cm^2/(Vs)$ in all our simulations unless otherwise specified. (a) Graphene absorption, from inset it is shown that graphene has remarkably high absorption at visible light range. (b) Permittivity of graphene. (c) SiC absorption and its Reststrahlen band. (d) Permittivity of SiC.

the zone where the graphene is suspended (see figure 1c).

We model the graphene optical properties using the local random phase approximation (RPA) model which is known to work well.[2,30] We also use the zero temperature limit which is a good approximation even for finite temperatures. The conductivity is given by

$$\sigma(\omega) = \frac{e^2 E_F}{\pi\hbar^2}\frac{i}{\omega + i\tau^{-1}} + \frac{e^2}{4\hbar^2}\left(\theta(\hbar\omega - 2E_F) + \frac{i}{\pi}\log\left(\left|\frac{\hbar\omega - 2E_F}{\hbar\omega + 2E_F}\right|\right)\right) \tag{1}$$

where τ is the carrier relaxation time and is linked to the carrier mobility μ via the equation $\tau = \frac{\mu E_F}{e v_F^2}$. θ denotes a step function and E_F is the Fermi energy. The first term describes intraband transitions and is Drude-like. This will dominate the response over the second term, which describes interband transitions, at the frequencies and levels of doping we consider. In figure 2a and 2b we plot the corresponding dielectric function for $E_F = 0.64\ eV$ and $\mu = 10000\ cm^2/(Vs)$ (which is a typical maximum value for the mobility of CVD grown

graphene) where it can be seen that graphene, for a single layer structure, has a remarkably large absorption at visible wavelengths.

The dielectric function for polar dielectrics like SiC can be described by a Lorentz oscillator model

$$\epsilon(\omega) = \epsilon_\infty \left(1 + \frac{\omega_{LO}^2 - \omega_{TO}^2}{\omega_{TO}^2 - \omega^2 - i\omega\gamma}\right) \tag{2}$$

which has a pole at the TO phonon frequency ω_{TO} and a zero-point crossing at ω_{LO}. For SiC[31] $\epsilon_\infty = 6.56$, $\omega_{LO} = 973\ cm^{-1}$, $\omega_{TO} = 797\ cm^{-1}$ and $\gamma = 4.76\ cm^{-1}$, in figure 2c and 2d we show the absorption and permittivity of SiC respectively. The SPhPs can only be supported in a narrow spectral bandwidth (in the case of SiC around 176 cm^{-1}) but crucially it corresponds to frequencies at which graphene plasmons can be excited: paving the way for interactions between the two types of excitations.

If the momentum mismatch is overcome, graphene SPPs can be excited by normal incident light. Assuming interband transitions can be ignored, the dispersion relation for the plasmon waves in a free standing graphene sheet is given by[30]

$$k_{spp}(\omega) = \frac{\pi\hbar^2\epsilon_0(\epsilon_1 + \epsilon_2)}{e^2 E_F}\left(1 + \frac{i}{\omega\tau}\right)\omega^2 \tag{3}$$

where k_{spp} is the in-plane wavevector of the plasmon and ϵ_1 and ϵ_2 are the relative permittivity of the materials in the infinite half-spaces above and below the graphene sheet. The dispersion is plotted in figure 3a for a graphene sheet in vacuum for different levels of doping, the dispersion curve indicates that the plasmons wavelength is on the order of 10-100 times smaller than the incident wavelength revealing the large confinement and the consequent momentum mismatch that must be overcome for efficient coupling. Unless otherwise specified, we use a Fermi energy of 0.64 eV throughout this work.

To investigate our system we begin by calculating the absorption of a SiC grating with no graphene sheet present. We assume that the SiC is infinitely thick below the grating to switch off the transmission channel and simplify analysis. We consider wavelengths and

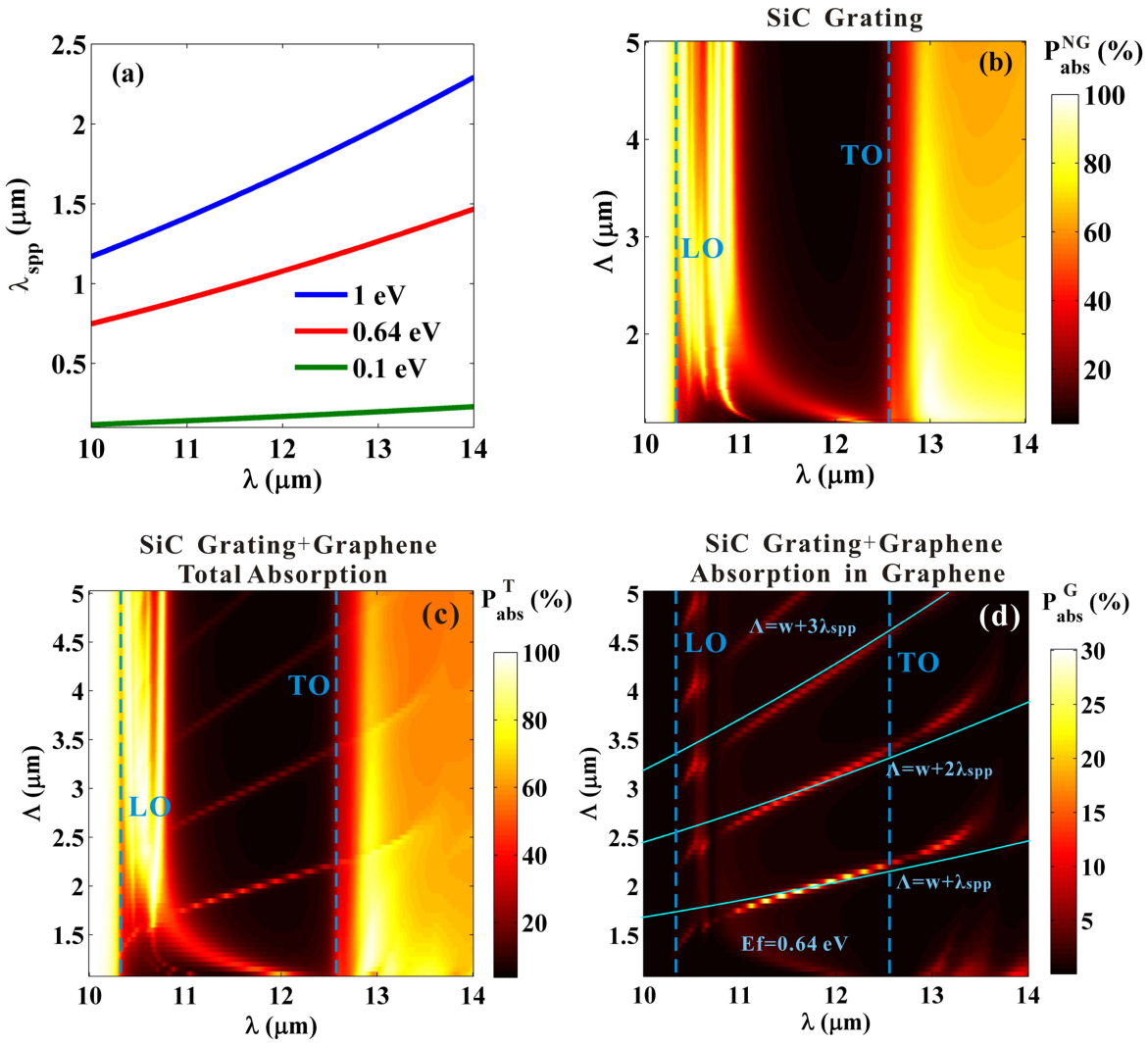

Figure 3: (a) Graphene SPP wavelength for different values of the chemical potential. (b) Total absorption (P_{abs}^{NG}) versus grating period (Λ) and incident wavelength (λ) for the SiC grating (with no graphene) structure for $w = h = 1\ \mu m$. (c) Total absorption (P_{abs}^{T}) versus grating period and incident wavelength for the SiC grating plus graphene structure for $w = h = 1\ \mu m$. (d) Graphene layer absorption (P_{abs}^{G}) versus grating period and incident wavelength the the SiC grating plus graphene structure for $w = h = 1\ \mu m$. The blue lines indicate a fit to a Fabry-Pérot model for a phase shift of $-\pi$ (see equation 4).

grating periods in the range 10 $\mu m \rightarrow$ 14 μm and 1.1 $\mu m \rightarrow$ 5 μm respectively with the grating height and ridge width are fixed at 1 μm. The results are shown in figure 3b. We see that within the Reststrahlen band there is now a number of peaks as compared to the plain SiC case (figure 2c), this is due to the interaction of the LO phonon and the grating allowing the excitation of LSPhPs.[13] There is a region of large absorption at the LSPhP

resonances, but elsewhere in the band the absorption is close to 0% as the SiC acts as a perfect reflector. Outside the Reststrahlen band, for frequencies less than ω_{LO} and larger than ω_{TO}, the absorption is very similar to that for a plain SiC surface shown in figure 2c.

Next we add graphene on top of the grating, with the results shown in figures 3c and

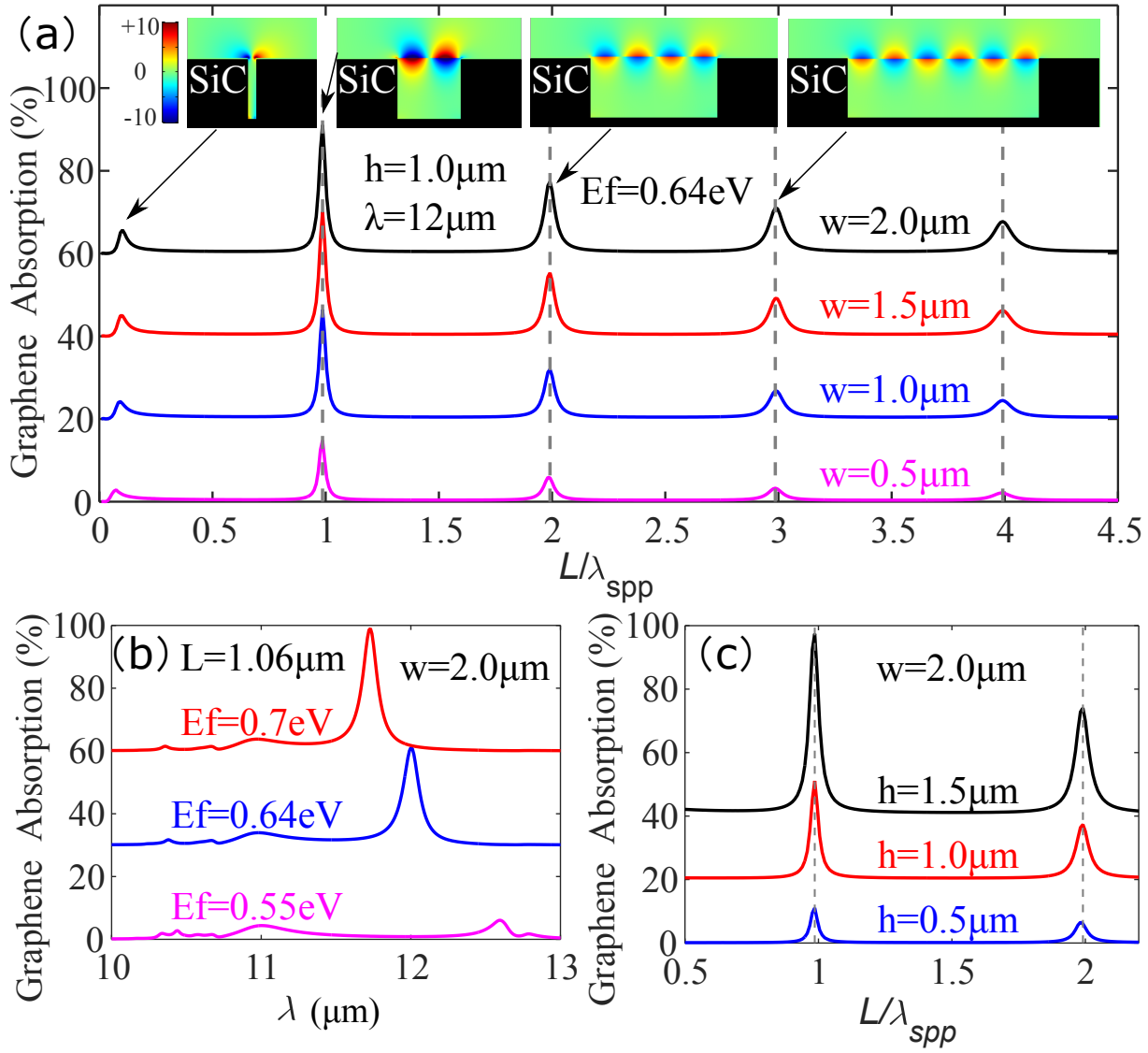

Figure 4: (a) Graphene layer's absorption at different geometric parameters L/λ_{spp} of the SiC grating. The peaks at integers numbers of L/λ_{spp} correspond to standing waves of the graphene SPPs as indicated by the above near field plot of E_y for each peak. The electric field (here normalised to the incident field magnitude) goes to zero at the boundaries meaning the plasmon modes must be antisymmetric. (b) The graphene layer absorption against excitation wavelength for fixed geometric parameters $L = 1.06\ \mu m$, $w = 2.0\ \mu m$ and $h = 1\ \mu m$. Shown for different Fermi energies. (c) The graphene layer absorption at different geometric parameters for different grating heights h and $E_F = 0.64\ eV$.

d. We consider two quantities: P_{abs}^{T}, which represents the total absorption (sum of the absorption of the SiC grating and the graphene layer) and P_{abs}^{G}, which is the absorption in the graphene. The most striking difference is the appearance of strong absorption peaks in the low absorbtion region of the Reststrahlen band for certain grating period lengths. This can be understood by looking at the near field of the y component of the electric field for each peak as shown in figure 4a. The field is concentrated in the graphene layer and has a fixed number of wavelengths in the region directly over air. The plasmon modes are antisymmetric, which is a consequence of the electric field boundary conditions. The normal incident field excites SPPs at the edge which are out of phase and will only constructively interfere for odd modes.[32] In the parts of the graphene that are located on top of the SiC there is a very weak field and (consequently low absorption). This can be understood by noting in this spectral region that the SiC acts, to a good approximation, as a perfect electrical conductor and screens out any external field very effectively. In other words, the field is zero outside the cavity region and leads to plasmon standing waves being established. To confirm this, in figure 4a we show the absorption varying with the cavity length (for a fixed wavelength $\lambda = 12\ \mu m$). We find at integer multiples of L/λ_{SPP} absorption peaks that correspond to the plasmon standing waves. This is shown pictorially in figure 1c. For non-normal incident light it is also possible to excite symmetric plasmon standing waves as the symmetry of the system is broken. Note that there is also a small peak located near $L/\lambda_{SPP} = 0$, which is a localised SPhP mode also visible without graphene (see figure 3b), it is present for small cavities due to near-field coupling between the two SiC slabs. Our findings have some similarities with earlier work on the plasmonic coupling between graphene SPPs and magnetic polaritons in silver gratings.[33] Note that the cavities used in that work are very deep (width of 300 nm and height of 2 μm) as compared to our system where the cavity height and width studied are always equal or comparable, which makes experimental realisation potentially much simpler. The highest field enhancement in our system is located on the graphene layer, which is very convenient for potential applications in molecular sensors. Note that the fact

the peak position does not change for varying Λ (for a fixed cavity length) is confirmation that these are localised cavity modes and not modes excited by diffraction effects due to the grating periodicity.[34] In an experiment it would be more natural to explore these standing wave modes by scanning the excitation light wavelength for a fixed geometric parameters, in figure 4b we show this for various chemical potentials for $L = 1.06\ \mu m$, $w = 2.0\ \mu m$ and $h = 1\ \mu m$. We find that as the Fermi energy is increased the absorption peak redshifts (as the SPP wavelength changes with E_F) and grows in intensity. This illustrates that our system can act as a tunable cavity thanks to the inclusion of the graphene sheet. In figure 4c we show how the grating height impacts the graphene absorption, we find that the absorption intensity is strongly dependent on the height. When the height is changed the graphene SPP wavelength does not change, this is because when h is large ($h > 500\ nm$ here) then equation 3 applies and λ_{SPP} depends only on the material directly above and below the suspended graphene (in this case air).

To confirm our intuition about these modes we use the graphene dispersion in equation 3 along with a Fabry-Pérot model

$$\delta\phi + \Re(k_{spp}(\omega))L = m\pi \tag{4}$$

where $\delta\phi$ is the phase shift. Taking a phase shift of $-\pi$ we find good agreement with the simulation results (see the blue lines in figure 3d) in the region near the TO energy where the grating acts as a perfect electric conductor (i.e. plasmon standing waves in the cavity). At frequencies away from this the simple model breaks downs as the phase shift is frequency dependent and will differ from $-\pi$. This is due to the grating not acting as a perfect reflector any more and allowing some field penetration into the SiC. To quantify the suitability of the cavity as an experimental system for strong light-matter interactions we consider the ratio Q/V. To calculate the volume we consider a square cavity (with sides of length L, we use $w = 1\ \mu m$ and L is calculated using a period Λ that sets up a plasmon standing wave) with a

plasmon standing wave setup in both directions, the dimension perpendicular to the graphene sheet is given by the out-of-plane decay of the plasmon $\sim 1/\Re[k_{spp}(\omega)]$[35] (as $k_{spp} >> 2\pi/\lambda$ then $k_z \sim ik_{spp}$, for 12 μm incident wavelength this distance corresponds to 0.17 μm). The quality factor can be estimated using $Q \approx \omega/\Delta\omega$ where we obtain the linewidth $\Delta\omega$ using a Lorentzian fit. At a wavelength of 12 μm we find a value of $Q/V = 8 \times 10^5/\lambda_0^3$ which is comparable to values found for other graphene nanoresonators.[4]

Another interesting feature, revealed in figure 3d (and a zoom-in is provided in figures

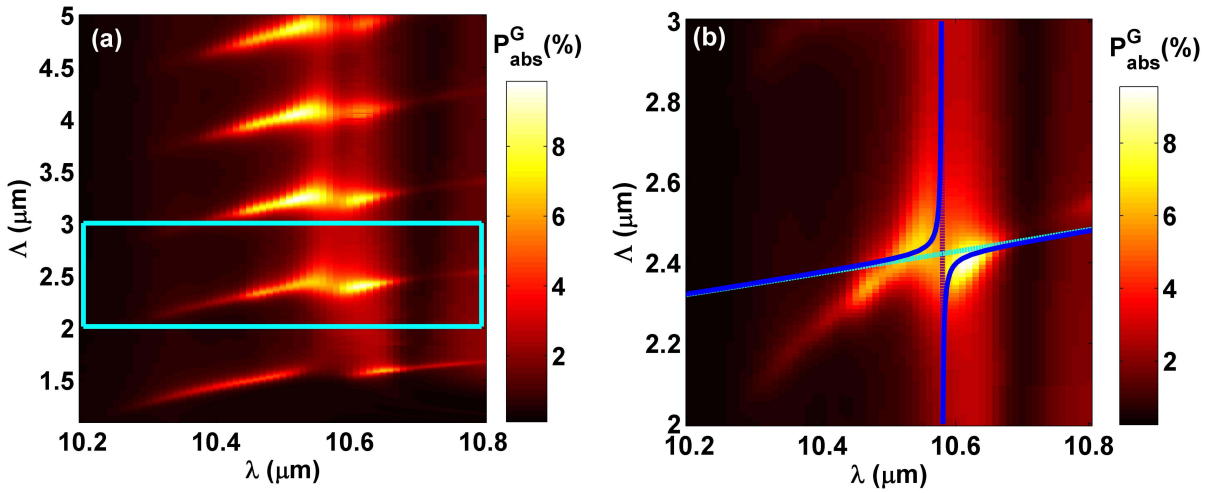

Figure 5: (a) Zoom in of the absorption in the graphene layers (for $w = h = 1$ μm) in the figure 3d between the wavelengths 10.2 and 10.8 μm highlighting the Rabi-splitting for different modes. (b) Zoom in for $m = 2$ mode, the purple dashed line indicates the LSPhP wavelength and the cyan dashed line shows the graphene SPP dispersion using the Fabry-Pérot model with a phase shift of -1.35π. The blue line shows the resulting splitting of the hybrid mode.

5a and b) is the presence of a anti-crossing point in the absorption spectrum close to the LO phonon frequency, this is a manifestation of strong coupling between two modes, the graphene plasmon and a localised cavity SPhP,[13] and can be intuitively understood by considering two coupled harmonic oscillators.[26] The shape of the Rabi splitting shown in figures 5a and b is a consequent of the dispersive graphene SPP (given by equation 4) and the LSPhP at a fixed wavelength of 10.6 μm. The strong coupling regime is very dependent on the level of the damping of the system, thus the small linewidths of graphene plasmons and SiC SPhPs is favourable for the observation of Rabi splitting. It should be noted that at frequencies

close to the LO phonon energy, graphene SPPs can become lossy due to substrate phonons.[4] In our cavity-grating system a substantial amount of the graphene is free-standing and not in contact with the substrate which should negate this.

In figure 6 we show a slice of the absorption in the graphene and apply a sum of two

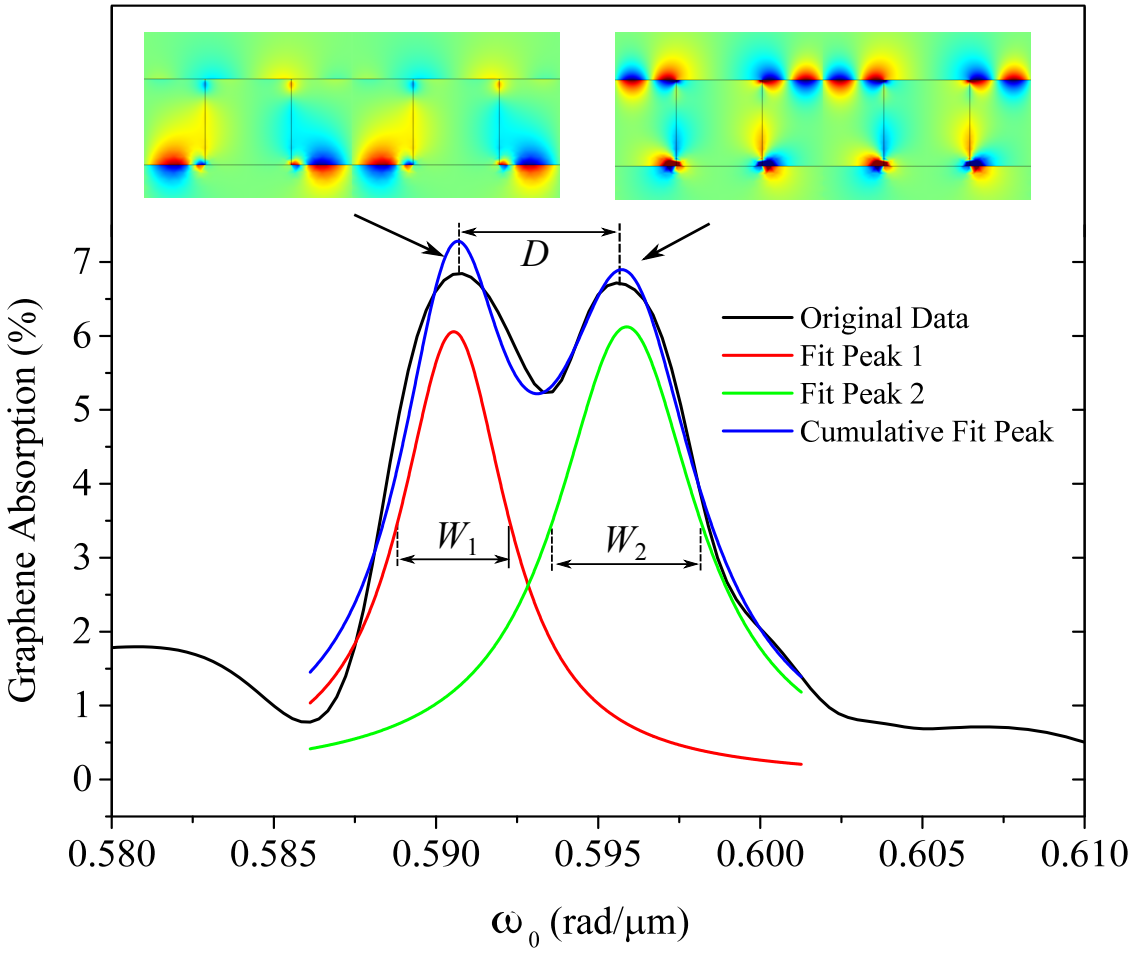

Figure 6: These spectra correspond to the $L = 1.45\mu m$, which means $\Lambda = 2.45\mu m$. The summation of two Lorentz equations is used to fit these peaks. The full widths at half maximum of these two peaks are 0.004 $rad/\mu m$ (W_1) and 0.005 $rad/\mu m$ (W_2), individually. The peak distance is $D = 0.005\ rad/\mu m$. The ratio $D/W = 1$ quantifies the strength of the coupling and shows that this is the strong coupling regime.

Lorentzian functions to fit the curve and quantify the strength of the coupling. We find the peak separation (i.e. the Rabi splitting) to be $\omega_R = 1\ meV$. This value can then be used

with a coupled harmonic oscillator model to describe the anti-crossing[36]

$$E_{\pm}(\omega) = \frac{\hbar\omega_{SPP} + \hbar\omega_{SPhP}}{2} \pm \frac{1}{2}\sqrt{(\hbar\omega_R)^2 + (\hbar\omega_{SPP} - \hbar\omega_{SPhP})^2} \tag{5}$$

where we take the the LSPhP energy to be fixed with a value of 0.12 eV and the graphene SPP dispersion is given by equations 3 and 4 and we use the phase shift as a fitting parameter as it can no longer be expected to be $-\pi$ at these wavelengths. The result for the fit to the $m = 2$ mode is shown in figure 5b where a good fit is obtained using a phase shift of $\delta\phi = -1.35\pi$, this indicates that at these frequencies the SiC does not act as a perfect reflector.

Also shown in figure 6 are two near field plots showing the different nature of the hybrid mode depending on the frequency, at lower frequencies the mode is more phonon-polariton-like and the absorption is situated at the bottom of the cavity. At larger frequencies the mode is more graphene-plasmon-like and the absorption is concentrated in the graphene layer on top. Thus over small frequency range one has a lot of spatial control of where absorption takes place in this system and is a consequence of strong coupling between modes. Further control of the relative contribution of each mode is given by cavity width and doping level. To quantify the coupling we compare the linewidth of the constituent modes (W_1 and W_2) to the splitting (D), for splitting to be experimentally observable $D \gtrsim W$.[26] Taking the largest linewidth we get a ratio of $D/W = 1$ which justifies considering this interaction of the two modes as strong coupling.

3 Conclusions

In conclusion we have studied a graphene and SiC cavity system and have shown its suitability as an experimentally realisable, tunable cavity that could be be useful for cavity quantum-electrodynamics and molecular sensing in the mid-IR. We have shown the inclusion of a graphene monolayer on a SiC grating leads to a number of new modes in the low absorption part of the Reststrahlen band. These modes can be explained as antisymmetric plasmon

standing waves set up by the SiC acting as a perfect conductor at these frequencies and are well explained by a simple Fabry-Pérot model. By altering the chemical potential of the graphene or changing the cavity width one could change the spectral position of these peaks: meaning we have a very tunable plasmonic cavity. Near to the LO phonon energy we find evidence of strong coupling between the graphene SPP and the localised SPhP leading to a hybrid mode[14] that exhibits characteristics of both constituent modes. Our results also offer promise that similar coupling with local trace level quantities of molecules could be possible. We find that over a small frequency range the spatial profile of the hybrid modes can change significantly. The tunability, high quality factor and low modal volume make this an ideal setup for molecular sensing and to study cavity-QED.

Acknowledgement

K.L. is supported by China Postdoctoral Science Foundation (No. 2014M560444), Collaborative Academic Training Program for Post-doctoral Fellows of Collaborative Innovation Center of Suzhou Nano Science and Technology. The work of J.M.F. was supported under a studentship from the Imperial College London funded by the EPSRC grant 1580548. X.X. is supported by Lee Family Scholars. S.M. acknowledges the Lee-Lucas Chair in Physics and the EPSRC Mathematical Fundamentals of Metamaterials Programme Grant (EP/L024926/1) and V.G. is acknowledging ONR Global funding (N62909-15-1-N082).

Author Information

Corresponding Authors

Email: xx2215@ic.ac.uk (X.X.)

Email: xfli@suda.edu.cn (X.L.)

Author Contributions

All authors have given approval to the final version of the manuscript.

Notes

The authors declare no competing financial interest.

References

(1) Novoselov, K. S.; Geim, A. K.; Morozov, S. V.; Jiang, D.; Zhang, Y.; Dubonos, S. V.; Grigorieva, I. V.; Firsov, A. A. Electric field effect in atomically thin carbon films. *science* **2004**, *306*, 666–669.

(2) Garcia de Abajo, F. J. Graphene plasmonics: challenges and opportunities. *ACS Photonics* **2014**, *1*, 135–152.

(3) Maier, S. A. *Plasmonics: fundamentals and applications*; Springer Science & Business Media, 2007.

(4) Brar, V. W.; Jang, M. S.; Sherrott, M.; Lopez, J. J.; Atwater, H. A. Highly confined tunable mid-infrared plasmonics in graphene nanoresonators. *Nano letters* **2013**, *13*, 2541–2547.

(5) Chen, C. F.; Park, C. H.; Boudouris, B. W.; Horng, J.; Geng, B. S.; Girit, C.; Zettl, A.; Crommie, M. F.; Segalman, R. A.; Louie, S. G.; Wang, F. Controlling inelastic light scattering quantum pathways in graphene. *Nature* **2011**, *471*, 617–620.

(6) Fei, Z. et al. Infrared nanoscopy of Dirac plasmons at the graphene–SiO2 interface. *Nano letters* **2011**, *11*, 4701–4705.

(7) Fei, Z.; Rodin, A. S.; Andreev, G. O.; Bao, W.; McLeod, A. S.; Wagner, M.; Zhang, L. M.; Zhao, Z.; Thiemens, M.; Dominguez, G.; Fogler, M. M.; Castro Neto, A. H.; Lau, C. N.; Keilmann, F.; Basov, D. N. Gate-tuning of graphene plasmons revealed by infrared nano-imaging. *Nature* **2012**, *487*, 82–85.

(8) Chen, J. N.; Badioli, M.; Alonso-Gonzalez, P.; Thongrattanasiri, S.; Huth, F.; Osmond, J.; Spasenovic, M.; Centeno, A.; Pesquera, A.; Godignon, P.; Elorza, A. Z.;

Camara, N.; de Abajo, F. J. G.; Hillenbrand, R.; Koppens, F. H. L. Optical nanoimaging of gate-tunable graphene plasmons. *Nature* **2012**, *487*, 77–81.

(9) Ju, L.; Geng, B. S.; Horng, J.; Girit, C.; Martin, M.; Hao, Z.; Bechtel, H. A.; Liang, X. G.; Zettl, A.; Shen, Y. R.; Wang, F. Graphene plasmonics for tunable terahertz metamaterials. *Nature nanotechnology* **2011**, *6*, 630–634.

(10) Shin, S.; Kim, N.; Kim, J.; Kim, K.; Noh, D.; Kim, K. S.; Chung, J. Control of the π plasmon in a single layer graphene by charge doping. *Applied Physics Letters* **2011**, *99*, 082110.

(11) Caldwell, J. D.; Lindsay, L.; Giannini, V.; Vurgaftman, I.; Reinecke, T. L.; Maier, S. A.; Glembocki, O. J. Low-loss, infrared and terahertz nanophotonics using surface phonon polaritons. *Nanophotonics* **2015**, *4*, 44–68.

(12) Caldwell, J. D.; Glembocki, O. J.; Francescato, Y.; Sharac, N.; Giannini, V.; Bezares, F. J.; Long, J. P.; Owrutsky, J. C.; Vurgaftman, I.; Tischler, J. G.; Wheeler, V. D.; Bassim, N. D.; Shirey, L. M.; Kasica, R.; Maier, S. A. Low-loss, extreme subdiffraction photon confinement via silicon carbide localized surface phonon polariton resonators. *Nano letters* **2013**, *13*, 3690–3697.

(13) Chen, Y. G.; Francescato, Y.; Caldwell, J. D.; Giannini, V.; Mass, T. W. W.; Glembocki, O. J.; Bezares, F. J.; Taubner, T.; Kasica, R.; Hong, M. H.; Maier, S. A. Spectral tuning of localized surface phonon polariton resonators for low-loss mid-IR applications. *ACS Photonics* **2014**, *1*, 718–724.

(14) Caldwell, J. D.; Vurgaftman, I.; Tischler, J. G.; Glembocki, O. J.; Owrutsky, J. C.; Reinecke, T. L. Atomic-scale photonic hybrids for mid-infrared and terahertz nanophotonics. *Nature nanotechnology* **2016**, *11*, 9–15.

(15) Liu, Y.; Willis, R. F. Plasmon-phonon strongly coupled mode in epitaxial graphene. *Physical Review B* **2010**, *81*, 081406.

(16) Koch, R.; Seyller, T.; Schaefer, J. Strong phonon-plasmon coupled modes in the graphene/silicon carbide heterosystem. *Physical Review B* **2010**, *82*, 201413.

(17) Yan, H.; Low, T.; Zhu, W.; Wu, Y.; Freitag, M.; Li, X.; Guinea, F.; Avouris, P.; Xia, F. Damping pathways of mid-infrared plasmons in graphene nanostructures. *Nature Photonics* **2013**, *7*, 394–399.

(18) Zhu, X.; Wang, W.; Yan, W.; Larsen, M. B.; Bøggild, P.; Pedersen, T. G.; Xiao, S.; Zi, J.; Mortensen, N. A. Plasmon–phonon coupling in large-area graphene dot and antidot arrays fabricated by nanosphere lithography. *Nano letters* **2014**, *14*, 2907–2913.

(19) Dai, S. et al. Graphene on hexagonal boron nitride as a tunable hyperbolic metamaterial. *Nature nanotechnology* **2015**, *10*, 682–686.

(20) Woessner, A.; Lundeberg, M. B.; Gao, Y.; Principi, A.; Alonso-GonzÃąlez, P.; Carrega, M.; Watanabe, K.; Taniguchi, T.; Vignale, G.; Polini, M.; Hone, J.; Hillenbrand, R.; Koppens, F. H. L. Highly confined low-loss plasmons in graphene-boron nitride heterostructures. *Nat Mater* **2015**, *14*, 421–425.

(21) Brar, V. W.; Jang, M. S.; Sherrott, M.; Kim, S.; Lopez, J. J.; Kim, L. B.; Choi, M.; Atwater, H. Hybrid surface-phonon-plasmon polariton modes in graphene/monolayer h-BN heterostructures. *Nano letters* **2014**, *14*, 3876–3880.

(22) Barcelos, I. D.; Cadore, A. R.; Campos, L. C.; Malachias, A.; Watanabe, K.; Taniguchi, T.; Maia, F. C.; Freitas, R.; Deneke, C. Graphene/h-BN plasmon–phonon coupling and plasmon delocalization observed by infrared nano-spectroscopy. *Nanoscale* **2015**, *7*, 11620–11625.

(23) Li, Y.; Yan, H.; Farmer, D. B.; Meng, X.; Zhu, W.; Osgood, R. M.; Heinz, T. F.; Avouris, P. Graphene plasmon enhanced vibrational sensing of surface-adsorbed layers. *Nano letters* **2014**, *14*, 1573–1577.

(24) Huck, C.; Vogt, J.; Neuman, T.; Nagao, T.; Hillenbrand, R.; Aizpurua, J.; Pucci, A.; Neubrech, F. Strong coupling between phonon-polaritons and plasmonic nanorods. *Optics Express* **2016**, *24*, 25528–25539.

(25) Li, X. F.; Yu, S. F. Modeling of Rabi splitting in quantum well microcavities using time-dependent transfer matrix method. *Optics Express* **2008**, *16*, 19285–19290.

(26) Törmä, P.; Barnes, W. L. Strong coupling between surface plasmon polaritons and emitters: a review. *Reports on Progress in Physics* **2015**, *78*, 013901.

(27) Kavokin, A.; Baumberg, J. J.; Malpuech, G.; Laussy, F. P. *Microcavities*; OUP Oxford, 2011; Vol. 16.

(28) Todisco, F.; Esposito, M.; Panaro, S.; De Giorgi, M.; Dominici, L.; Ballarini, D.; Fernández-Domínguez, A. I.; Tasco, V.; Cuscunà, M.; Passaseo, A.; Ciracì, C.; Gigli, G.; Sanvitto, D. Toward Cavity Quantum Electrodynamics with Hybrid Photon Gap-Plasmon States. *ACS Nano* **2016**, *10*, 11360–11368, PMID: 28024373.

(29) Francescato, Y.; Giannini, V.; Yang, J.; Huang, M.; Maier, S. A. Graphene sandwiches as a platform for broadband molecular spectroscopy. *ACS Photonics* **2014**, *1*, 437–443.

(30) Koppens, F. H.; Chang, D. E.; García de Abajo, F. J. Graphene plasmonics: a platform for strong light–matter interactions. *Nano letters* **2011**, *11*, 3370–3377.

(31) Francescato, Y. New frequencies and geometries for plasmonics and metamaterials. Ph.D. thesis, Imperial College London, 2014.

(32) Du, L.; Tang, D.; Yuan, X. Edge-reflection phase directed plasmonic resonances on graphene nano-structures. *Optics express* **2014**, *22*, 22689–22698.

(33) Zhao, B.; Zhang, Z. M. Strong plasmonic coupling between graphene ribbon array and metal gratings. *ACS Photonics* **2015**, *2*, 1611–1618.

(34) Rivas, J. G.; Vecchi, G.; Giannini, V. Surface plasmon polariton-mediated enhancement of the emission of dye molecules on metallic gratings. *New Journal of Physics* **2008**, *10*, 105007.

(35) Giannini, V.; Zhang, Y.; Forcales, M.; Rivas, J. G. Long-range surface polaritons in ultra-thin films of silicon. *Optics express* **2008**, *16*, 19674–19685.

(36) Schlather, A. E.; Large, N.; Urban, A. S.; Nordlander, P.; Halas, N. J. Near-field mediated plexcitonic coupling and giant Rabi splitting in individual metallic dimers. *Nano letters* **2013**, *13*, 3281–3286.

Graphical TOC Entry